A Design of Novel Grooved Circular Waveguide Polarizers

Naofumi Yoneda, *Member, IEEE*, Moriyasu Miyazaki, *Senior Member, IEEE*, Hiroyuki Matsumura, and Masao Yamato

***Abstract*—This paper presents novel types of polarizers that are composed of grooved circular waveguides. The presented polarizers are suitable for realizing high-performance and low-fabrication cost in the Ka-band and above because of simple structure. Accurate analysis and design of the polarizers are performed using full-wave mode-matching techniques applied to the circular-to-rectangular waveguide T-junctions and cross-junctions. Ka-band grooved circular waveguide polarizers fabricated with the aid of the analysis and design techniques have realized excellent performance without tuning elements.**

***Index Terms*—Mode-matching methods, polarizers, waveguides.**

I. Introduction

IN CIRCULARLY polarized antenna feed systems, polarizers are used to convert linearly polarized signals provided at the first interface port (e.g., a circular or square waveguide) into circularly polarized signals supplied to the second interface port (i.e., the antenna interface port). Typical examples of polarizer type that aim at high performance and compact size are a circular waveguide polarizer with metallic posts, a corrugated waveguide polarizer, and a dielectric-slab waveguide polarizer [1], [2]. In the Ka-band and above, however, these polarizer types have serious degradation in performance due to manufacturing inaccuracy and difficulty of setting up tuning devices, as the dimensions of waveguide cross sections should be designed very small to avoid excitation of higher order propagation modes. Consequently, for polarizers operated in the Ka-band and above, low complexity of the physical structure is required to reduce influence of manufacturing inaccuracy. In addition, the design is in need of an accurate analysis to realize high performance without tuning elements.

In this paper, we present novel types of polarizers that are composed of grooved circular waveguides. The presented polarizers are suitable for realizing high-performance and low-fabrication cost in the Ka-band and above because of simple structure without corrugated components, metallic posts, and a dielectric slab taper. We further propose a convenient design method of the grooved circular waveguide polarizers, which applies the well-known design method of the branch waveguide coupler [3], [4]. The design method is accurately performed using full-wave mode-matching techniques for circular-to-rectangular waveguide T-junctions and cross junctions [5]. Ka-band grooved circular waveguide polarizers fabricated with the aid of analysis and design techniques have realized excellent performance without tuning elements.

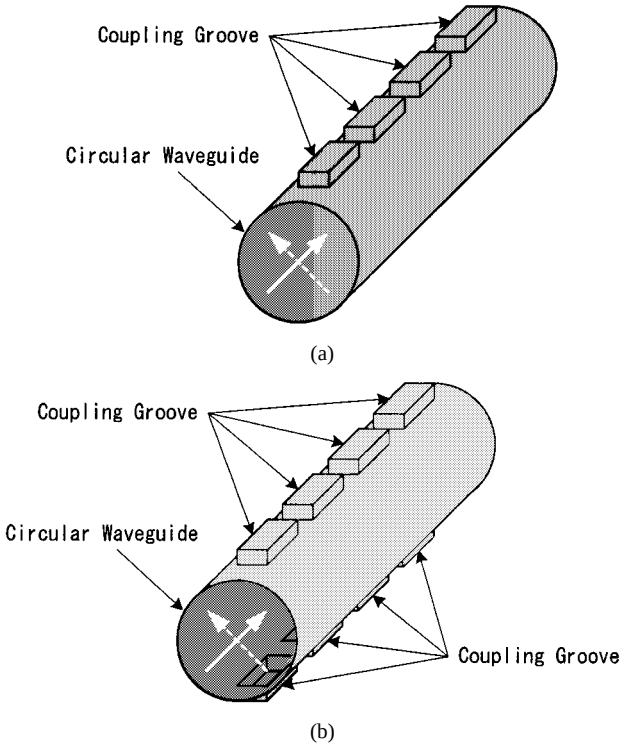

Fig. 1. (a) Single-grooved circular waveguide polarizer. (b) Double-grooved circular waveguide polarizer.

II. Configuration

Fig. 1 depicts the structure of two proposed polarizers with four grooved circular waveguides. Type number one is a single-grooved circular waveguide polarizer shown in Fig. 1(a). The polarizer is composed of a circular common waveguide and several grooves arranged in a single line. Type number two is a double-grooved circular waveguide polarizer shown in Fig. 1(b). The polarizer is composed of a circular common waveguide and several grooves aligned diagonally with regard to the circular waveguide cross section. Both of the polarizers have the advantage of reducing the degradation in antenna feed performance due to manufacturing inaccuracy because they have coupling grooves in the sparse electromagnetic

Manuscript received March 6, 2000; revised August 22, 2000.

N. Yoneda and M. Miyazaki are with the Information Technology Research and Development Center, Mitsubishi Electric Corporation, Kamakura 247-8501, Japan.

H. Matsumura is with the Mitsubishi Electric Engineering Corporation, Kamakura 247-8520, Japan.

M. Yamato is with the Kamakura Works, Mitsubishi Electric Corporation, Kamakura 247-8520, Japan.

Publisher Item Identifier S 0018-9480(00)10772-0.

0018–9480/00$10.00 © 2000 IEEE

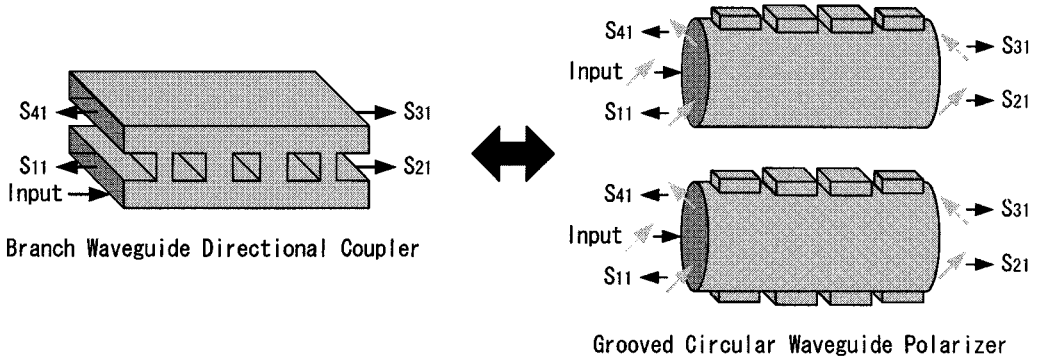

Fig. 2. Design concept of grooved circular waveguide polarizer.

field (i.e., in the wall of the circular waveguide) instead of arranging salient features and dielectric slabs in the dense electromagnetic field (i.e., inside of the circular waveguide). Respectively, by deciding the size and spacing of the grooves according to the design method discussed below, the incident linearly polarized modes that exhibit $\pm 45^\circ$ offset with respect to the diagonal alignment of grooves can be converted into right- and left-hand-side circularly polarized output wave. The single-grooved circular waveguide polarizer is suitable for realizing the small cross section of the common waveguide as compare with the double-grooved circular waveguide polarizer. On the other hand, the double-grooved circular waveguide polarizer is suitable for realizing the large cross section of the common waveguide (i.e., short waveguide wavelength) and reducing the component size in the direction of the longitudinal axis of the common waveguide because the symmetric structure enables the polarizer to suppress excitation of higher order propagation modes.

III. Design and Analysis

In a circular waveguide, a circularly polarized wave is represented by the superposition of orthogonal dual-polarized TE_{11} circular waveguide mode, thus, the presented polarizers can be treated as electrically four-port device with respect to the orthogonal dominant modes. Here, on the occasion of incident, a dominant mode to the four-port device, low return loss, high isolation between two orthogonal modes at input port, 3-dB power splitting and 90° differential phase shifting between two orthogonal modes at the output port are in demand for polarizer performance. Therefore, it is considered that the well-known design method of the branch waveguide 3-dB directional coupler can be applied to the design of the polarizers [3], [4]. Fig. 2 illustrates the design concept of the grooved circular waveguides. According to the design of the 3-dB directional coupler with n-branches, each size of the groove is determined by satisfying the following coupling characteristics:

$$A_1 = 2Z_1/(4+Z_1^2) \tag{1}$$

$$A_2 = 2Z_2/(4+Z_2^2) \tag{2}$$

where A_1 is each scattering parameter S_{31} (i.e., coupling voltage amplitude) of two end grooved waveguides, Z_1 is the corrected end branch guide impedance, A_2 is each scattering parameter S_{31} of the $n-2$ center connecting grooved waveguides, and Z_2 is the corrected center branch guide impedance. Corrected branch guide impedance Z_1 and Z_2 are solutions for the 3-dB directional coupler with n-branches, which give a perfect input match at the center frequency within the assigned operating band [3]. Furthermore, each space between grooved waveguide centers L is determined by

$$L \approx (2n+1)\lambda_g/4, \qquad n \geq 0 \tag{3}$$

where λ_g is the common circular waveguide wavelength of the fundamental mode at the center frequency. This design method is accomplished by equating numerically obtained coupling characteristics of grooved circular waveguides in the following full-wave analysis to the above-mentioned coupling characteristics of branch waveguides.

As shown in Fig. 1, the single-grooved circular waveguide is composed of two key building-block elements, i.e., a circular-to-rectangular waveguide T-junction and a short-circuit rectangular waveguide. We can realize an accurate design of the polarizer using full-wave analysis of circular-to-rectangular waveguide H- and E-plane T-junctions associated with the generalized S-matrix technique [5]. The full-wave analysis has the capability of including high-order mode influences and the advantage of shortening the computing time as compared with the finite-element method. On the other hand, the double-grooved circular waveguide is composed of two key-building block elements, i.e., a circular-to-rectangular waveguide cross junction and two short-circuit rectangular waveguides. We perform an accurate design of the presented polarizer using full-wave analysis of circular-to-rectangular waveguide H- and E-plane cross junctions, which expands the mode-matching method for circular-to-rectangular waveguide H-/E-plane T-junctions [5]. Fig. 3 shows the concept and coordinate system for modeling a circular-to-rectangular waveguide H- and E-plane cross junction. A discontinuity is given by the link of a circular waveguide to a parallel-plate radial waveguide junction and a radial cavity with two rectangular waveguides [5]. For example, by the application of the resonator method [6], the electromagnetic fields in regions (1)–(5) of the H-plane cross junction, shown in Fig. 3, are derived from the following

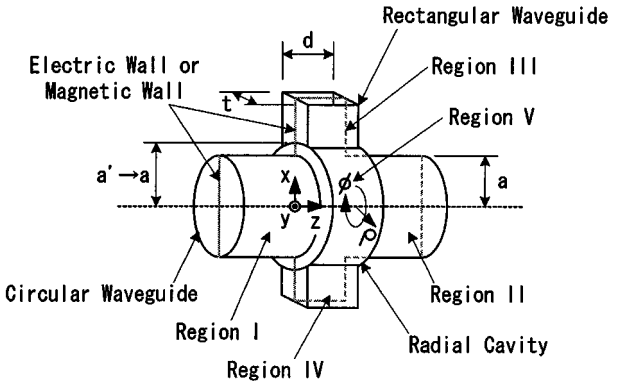

Fig. 3. Circular-to-rectangular waveguide cross junction; concept of analysis and coordinate systems.

z-component of vector potentials $A_e^{(i)}$ and $A_h^{(i)}$:

$$A_{ez}^{(1)} = \sum_q^Q \sum_l^L G_{eql}^{(1)} \cdot J_l\left(\frac{\chi_{lq}}{a}\rho\right) \cdot \sin l\phi \cdot \left(F_{eql}^{(1)} \cdot e^{-jk_{zeql}^{(1)}z} - B_{eql}^{(1)} \cdot e^{+jk_{zeql}^{(1)}z}\right)$$

$$A_{hz}^{(1)} = \sum_q^Q \sum_l^L G_{hql}^{(1)} \cdot J_l\left(\frac{\chi'_{lq}}{a}\rho\right) \cdot \cos l\phi \cdot \left(F_{hql}^{(1)} \cdot e^{-jk_{zhql}^{(1)}z} + B_{hql}^{(1)} \cdot e^{+jk_{zhql}^{(1)}z}\right) \quad (4)$$

$$A_{ez}^{(2)} = \sum_q^Q \sum_l^L G_{eql}^{(2)} \cdot J_l\left(\frac{\chi_{lq}}{a}\rho\right) \cdot \sin l\phi \cdot \left(F_{eql}^{(2)} \cdot e^{-jk_{zeql}^{(2)}(z-d)} - B_{eql}^{(2)} \cdot e^{+jk_{zeql}^{(2)}(z-d)}\right)$$

$$A_{hz}^{(2)} = \sum_q^Q \sum_l^L G_{hql}^{(2)} \cdot J_l\left(\frac{\chi'_{lq}}{a}\rho\right) \cdot \cos l\phi \cdot \left(F_{hql}^{(2)} \cdot e^{-jk_{zeql}^{(2)}(z-d)} + B_{hql}^{(2)} \cdot e^{+jk_{zhql}^{(2)}(z-d)}\right) \quad (5)$$

$$A_{ez}^{(3)} = \sum_m^M \sum_n^N G_{emn}^{(3)} \cdot \sin\frac{2m\pi y}{t} \cdot \cos\frac{n\pi z}{d} \cdot \left(F_{emn}^{(3)} \cdot e^{-jk_{xenm}^{(3)}(x-a)} - B_{emn}^{(3)} \cdot e^{+jk_{xenm}^{(3)}(x-a)}\right)$$

$$A_{hz}^{(3)} = \sum_m^M \sum_n^N G_{hmn}^{(3)} \cdot \cos\frac{2m\pi y}{t} \cdot \sin\frac{n\pi z}{d} \cdot \left(F_{hmn}^{(3)} \cdot e^{-jk_{xhmn}^{(3)}(x-a)} + B_{hmn}^{(3)} \cdot e^{+jk_{xhmn}^{(3)}(x-a)}\right) \quad (6)$$

$$A_{ez}^{(4)} = \sum_m^M \sum_n^N G_{emn}^{(4)} \cdot \sin\frac{2m\pi y}{t} \cdot \cos\frac{n\pi z}{d} \cdot \left(F_{emn}^{(4)} \cdot e^{-jk_{xemn}^{(4)}(x+a)} - B_{emn}^{(4)} \cdot e^{+jk_{xemn}^{(4)}(x+a)}\right)$$

$$A_{hz}^{(4)} = \sum_m^M \sum_n^N G_{hmn}^{(4)} \cdot \cos\frac{2m\pi y}{t} \cdot \sin\frac{n\pi z}{d} \cdot \left(F_{xhmn}^{(4)} \cdot e^{-jk_{xhmn}^{(4)}(x+a)} + b_{xhmn}^{(4)} \cdot e^{+jk_{xhmn}^{(4)}(x+a)}\right) \quad (7)$$

$$A_{ez}^{(5)} = \sum_q^Q \sum_l^L C_{eql}^{(1)} \cdot J_l\left(\frac{\chi_{lq}}{a}\rho\right) \cdot \sin l\phi \cdot \cos\left\{k_{zeql}^{(1)}(d-z)\right\} + \sum_q^Q \sum_l^L C_{eql}^{(2)} \cdot J_l\left(\frac{\chi_{lq}}{a}\rho\right) \cdot \sin l\phi \cdot \cos\left(k_{zeql}^{(2)}z\right) + \sum_n^N \sum_l^L C_{enl}^{(5)} \cdot J_l(k_{\rho en}^{(5)}\rho) \cdot \sin l\phi \cdot \cos\frac{n\pi z}{d}$$

$$A_{hz}^{(5)} = \sum_q^Q \sum_l^L C_{hql}^{(1)} \cdot J_l\left(\frac{\chi'_{lq}}{a}\rho\right) \cdot \cos l\phi \cdot \sin\left\{k_{zhql}^{(1)}(d-z)\right\} + \sum_q^Q \sum_l^L C_{hql}^{(2)} \cdot J_l\left(\frac{\chi'_{lq}}{a}\rho\right) \cdot \cos l\phi \cdot \sin\left(k_{zhql}^{(2)}z\right) + \sum_n^N \sum_l^L C_{hnl}^{(5)} \cdot J_l(k_{\rho hn}^{(5)}\rho) \cdot \cos l\phi \cdot \sin\frac{n\pi z}{e} \quad (8)$$

where $G_{eql}^{(i)}$ and $G_{hql}^{(i)}$ ($i = 1$ or 2) are normalization terms of TM_{ql} and TE_{ql} modes in circular waveguide, $G_{emn}^{(i)}$ and $G_{hmn}^{(i)}$ ($i = 3$ or 4) are normalization terms of TM_{mn}^z and TE_{mn}^z modes (i.e., hybrid modes [8]) in rectangular waveguide, $k_{zeql}^{(i)}$ and $k_{zhql}^{(i)}$ are propagation constants of TM_{ql} and TE_{ql} modes, $k_{xemn}^{(i)}$ and $k_{xhmn}^{(i)}$ are propagation constants of TM_{mn}^z and TE_{mn}^z modes, $k_{\rho en}^{(5)}$ and $k_{\rho hn}^{(5)}$ are propagation constants of TM_{nl} and TE_{nl} modes in parallel-plate radial waveguide, $F_{eql}^{(i)}$, $F_{hql}^{(i)}$, $F_{emn}^{(i)}$, $F_{hmn}^{(i)}$, $B_{eql}^{(i)}$, $B_{hql}^{(i)}$, $B_{emn}^{(i)}$, and $B_{hmn}^{(i)}$ are amplitude vectors of the forward and backward waves, $C_{eql}^{(i)}$, $C_{hql}^{(i)}$, $C_{enl}^{(5)}$, and $C_{hnl}^{(5)}$ are the unknown coefficients that can be expressed as a function of the above normalization terms, propagation constants, and amplitude vectors. Similarly, the electromagnetic fields in respective regions of the E-plane cross junction shown in Fig. 3 are derived from the following z-component of vector potentials $A_e^{(i)}$ and $A_h^{i)}$:

$$A_{ez}^{(1)} = \sum_q^Q \sum_l^L G_{eql}^{(1)} \cdot J_l\left(\frac{\chi_{lq}}{a}\rho\right) \cdot \cos l\phi \cdot \left(F_{eql}^{(1)} \cdot e^{-jk_{zeql}^{(1)}z} - B_{eql}^{(1)} \cdot e^{j k_{zeql}^{(1)}z}\right)$$

$$A_{hz}^{(1)} = \sum_q^Q \sum_l^L G_{hql}^{(1)} \cdot J_l\left(\frac{\chi'_{lq}}{a}\rho\right) \cdot \sin l\phi \cdot \left(F_{hql}^{(1)} \cdot e^{-jk_{zhql}^{(1)}z} + B_{hql}^{(1)} \cdot e^{+jk_{zhql}^{(1)}z}\right) \quad (9)$$

$$A_{ez}^{(2)} = \sum_q^Q \sum_l^L G_{eql}^{(2)} \cdot J_l\left(\frac{\chi_{lq}}{a}\rho\right) \cdot \cos l\phi \cdot \left(F_{eql}^{(2)} \cdot e^{-jk_{zeql}^{(2)}(z-d)} - B_{eql}^{(2)} \cdot e^{+jk_{zeql}^{(2)}(z-d)}\right)$$

$$A_{hz}^{(2)} = \sum_q^Q \sum_l^L G_{hql}^{(2)} \cdot J_l\left(\frac{\chi'_{lq}}{a}\rho\right) \cdot \sin l\phi \cdot \left(F_{hql}^{(2)} \cdot e^{-jk_{zhql}^{(2)}(z-d)} + B_{hql}^{(2)} \cdot e^{+jk_{zhql}^{(2)}(z-d)}\right) \quad (10)$$

$$A_{ez}^{(3)} = \sum_{m}^{M}\sum_{n}^{N} G_{emn}^{(3)} \cdot \cos\frac{(2m+1)\pi y}{t} \cdot \cos\frac{n\pi z}{d} \cdot (F_{emn}^{(3)} \cdot e^{-jk_{emn}^{(3)}(x-a)} - B_{emn}^{(3)} \cdot e^{+jk_{xemn}^{(3)}(x-a)})$$

$$A_{hz}^{(3)} = \sum_{m}^{M}\sum_{n}^{N} G_{hmn}^{(3)} \cdot \sin\frac{(2m+1)\pi y}{t} \cdot \sin\frac{n\pi z}{d} \cdot \left(F_{hmn}^{(3)} \cdot e^{-jk_{xhmn}^{(3)}(x-a)} + B_{hmn}^{(3)} \cdot e^{+jk_{xhmn}^{(3)}(x-a)}\right) \quad (11)$$

$$A_{ez}^{(4)} = \sum_{m}^{M}\sum_{n}^{N} G_{emn}^{(4)} \cdot \cos\frac{(2m+1)\pi y}{t} \cdot \cos\frac{n\pi z}{d} \cdot \left(F_{emn}^{(4)} \cdot e^{-jk_{xemn}^{(4)}(x+a)} - B_{emn}^{(4)} \cdot e^{+jk_{xemn}^{(4)}(x+a)}\right)$$

$$A_{hz}^{(4)} = \sum_{m}^{M}\sum_{n}^{N} G_{hmn}^{(4)} \cdot \sin\frac{(2m+1)\pi y}{t} \cdot \sin\frac{n\pi z}{d} \cdot \left(F_{hmn}^{(4)} \cdot e^{-jk_{xhmn}^{(4)}(x+a)} + B_{hmn}^{(4)} \cdot e^{+jk_{xhmn}^{(4)}(x+a)}\right) \quad (12)$$

$$A_{ez}^{(5)} = \sum_{q}^{Q}\sum_{l}^{L} C_{eql}^{(1)} \cdot J_l\left(\frac{\chi_{lq}}{a}\rho\right) \cdot \cos l\phi \cdot \cos\left\{k_{zeql}^{(1)}(d-z)\right\} + \sum_{q}^{Q}\sum_{l}^{L} C_{eql}^{(2)} \cdot J_l\left(\frac{\chi_{lq}}{a}\rho\right) \cdot \cos l\phi \cdot \cos\left(k_{zeql}^{(2)}z\right) + \sum_{n}^{N}\sum_{l}^{L} C_{enl}^{(5)} \cdot J_l(k_{\rho en}^{(5)}\rho) \cdot \cos l\phi \cdot \cos\frac{n\pi z}{d}$$

$$A_{hz}^{(5)} = \sum_{q}^{Q}\sum_{l}^{L} C_{hql}^{(1)} \cdot J_l\left(\frac{\chi'_{lq}}{a}\rho\right) \cdot \sin l\phi \cdot \sin\left\{k_{zhql}^{(1)}(d-z)\right\} + \sum_{q}^{Q}\sum_{l}^{L} C_{hql}^{(2)} \cdot J_l\left(\frac{\chi'_{lq}}{a}\rho\right) \cdot \sin l\phi \cdot \sin\left(k_{zhql}^{(2)}z\right) + \sum_{n}^{N}\sum_{l}^{L} C_{hnl}^{(5)} \cdot J_l(k_{\rho hn}^{(5)}\rho) \cdot \sin l\phi \cdot \sin\frac{n\pi z}{d}. \quad (13)$$

By matching the derived field components at the four interfaces between the above regions, the generalized scattering matrices of the circular-to-rectangular waveguide H-/E-plane cross junctions are, respectively, obtained [5]–[7].

Fig. 4 shows the concept for full-wave analysis of grooved circular waveguides. The scattering coefficients S_{11}, S_{21}, S_{31}, and S_{41} of grooved circular waveguides are, respectively, expressed as follows when the incident linearly polarized TE_{11} modes exhibit $\pm 45^\circ$ offset with respect to the diagonal alignment of grooves:

$$S_{11} = S'_{11}/2 + S''_{11}/2 \quad (14)$$

$$S_{21} = S'_{21}/2 + S''_{21}/2 \quad (15)$$

$$S_{31} = S'_{21}/2 - S''_{21}/2 \quad (16)$$

$$S_{41} = S'_{11}/2 - S''_{11}/2 \quad (17)$$

where S'_{11} are reflection coefficients at input port of the H-plane T-junction/cross junctions with short-circuit rectangular waveguides, S'_{21} are transmission coefficients between the input and output ports of the same H-plane T-junction/cross junctions, S''_{11} are reflection coefficients at input port of E-plane T-junction/cross junctions with short-circuit rectangular waveguides, and S''_{21} are transmission coefficients between the input and output ports of the same E-plane T-junction/cross junctions. Therefore, analysis and design of the grooved circular waveguides are performed by combining the derived generalized scattering matrices of H-/E-plane T-junction/cross junctions and well-known scattering matrices of short-circuit rectangular waveguide. Similarly, analyses of grooved circular waveguide polarizers are realized by cascading the above-mentioned scattering matrices.

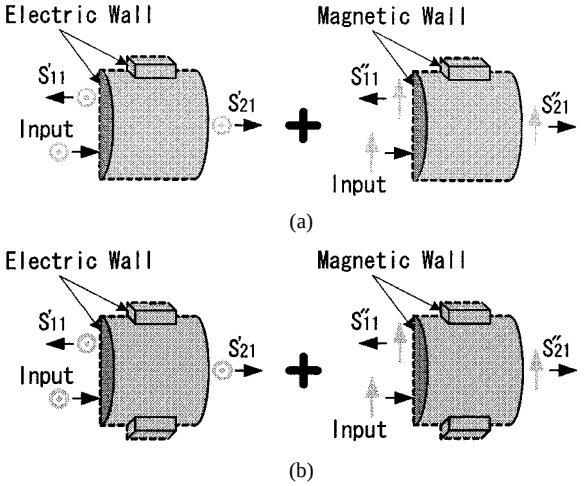

Fig. 4. Concept of analysis for grooved circular waveguides. (a) Single-grooved circular waveguide. (b) Double-grooved circular waveguide.

As typical design examples, a polarizer with four single-grooved circular waveguides and a polarizer with four double-grooved circular waveguides are designed in 20-GHz band with the aid of the presented design and analysis techniques. The total length of the designed single-grooved circular waveguide polarizer is 75 mm, and the diameter of the circular common waveguide is 10 mm. The size of two end grooves and two center grooves are W: 0.3 mm $*$ L: 14.8 mm $*$ D: 3.4 mm/W: 0.7 mm $*$ L: 14.8 mm $*$ D: 0.3 mm, and the space between grooved waveguide centers grooves is 20 mm ($\approx 3\lambda_g/4$). On the other hand, the total length of the designed double-grooved circular waveguide polarizer is 55 mm, and the diameter of the circular common waveguide is 13 mm. The size of two end grooves and two center grooves are W: 1.7 mm $*$ L: 11.7 mm $*$ D: 2.6 mm/W: 4.6 mm $*$ L: 11.7 mm $*$ D: 2.8 mm, and the space between grooved waveguide centers grooves is 14 mm ($\approx 3\lambda_g/4$). Fig. 5 shows the computed characteristics of the designed grooved circular waveguide polarizers. The calculated results indicate that a good match and a pure circular polarization can be obtained using the simple structure of the presented grooved circular waveguide polarizers and the above-mentioned design method.

IV. Experimental Result

A 20-GHz-band double-grooved circular waveguide polarizer and a 30-GHz-band double-grooved circular waveguide polarizer have been fabricated with the aid of the

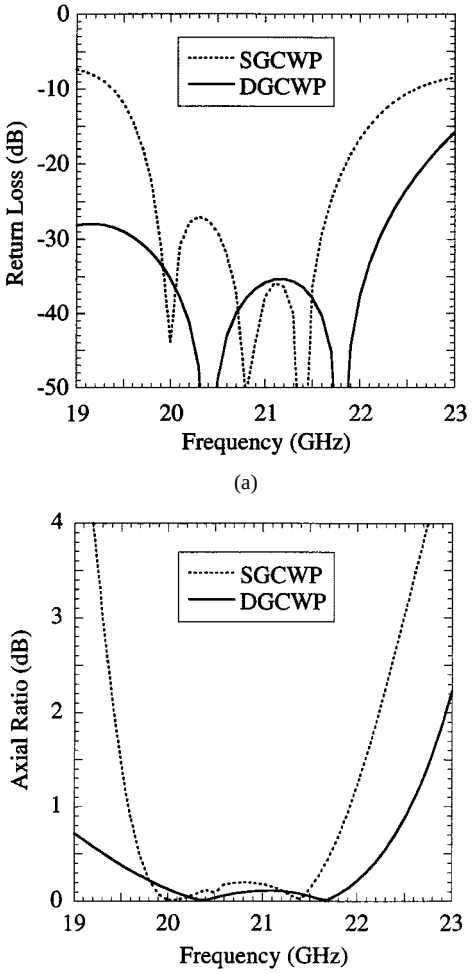

Fig. 5. Calculated characteristics of the 20-GHz-band grooved circular waveguide polarizers. SGCWP: single-grooved circular waveguide. DGCWP: double-grooved circular waveguide. (a) Return loss. (b) Axial ratio.

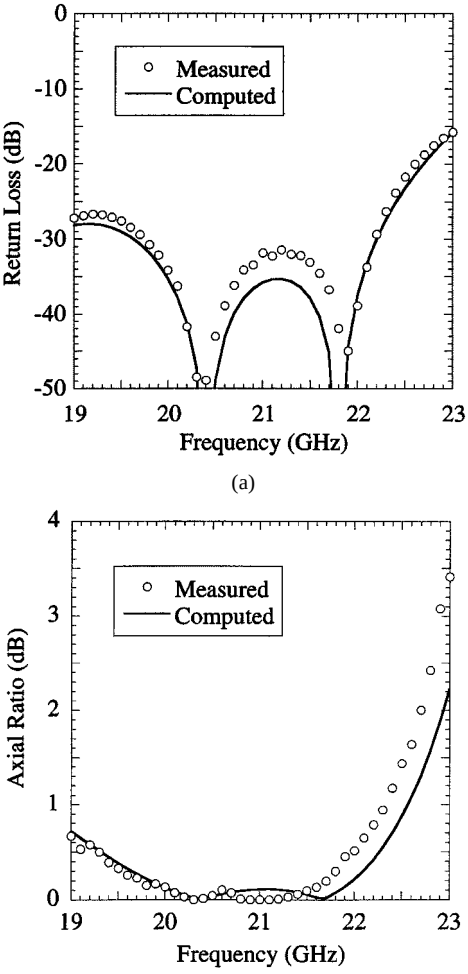

Fig. 7. Measured and calculated characteristics of the 20-GHz-band grooved circular waveguide polarizer. (a) Return loss. (b) Axial ratio.

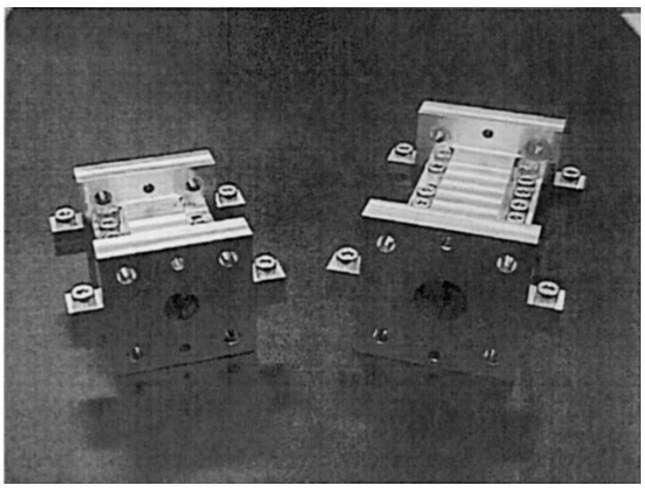

Fig. 6. 20- and 30-GHz-band double-grooved circular waveguide polarizers.

above-mentioned design and analysis techniques. Fig. 6 shows a photograph of the fabricated polarizers. Both of the polarizers are composed of four double-grooved circular waveguides. The 20-GHz-band polarizer is designed to provide a good match (voltage standing wave ratio (VSWR) $<$ 1.06) and a pure circular polarization (axial ratio $<$ 0.3 dB) over the frequency range between 20.0–21.5 GHz. The total length of the designed polarizer is 55 mm, and the diameter of the circular common waveguide is 13 mm. The size of two end grooves and two center grooves are W: 1.7 mm $*$ L: 11.7 mm $*$ D: 2.6 mm/W: 4.6 mm $*$ L: 11.7 mm $*$ D: 2.8 mm, respectively, and the space between grooved waveguide centers grooves is 14 mm ($\approx 3\lambda_g/4$). The 30-GHz-band polarizer is designed to obtain high performance (VSWR $<$ 1.06, axial ratio $<$ 0.5 dB) over the frequency range between 29.0– 32.0 GHz. The total length of the designed polarizer is 40 mm, and the diameter of the circular common waveguide is 9 mm. The size of two end grooves and two center grooves are W: 1.1 mm $*$ L: 8.1 mm $*$ D: 1.8 mm/W: 3.2 mm $*$ L: 8.1 mm $*$ D: 1.9 mm, respectively, and the space between grooved waveguide centers grooves is 9 mm ($\approx 3\lambda_g/4$). Figs. 7 and 8 show the reflection and axial ratio characteristics of the 20-GHz band and 30-GHz-band grooved circular waveguide polarizers. A good agreement is obtained between the experimental and calculated data both in Figs. 7 and 8. The fabricated 20-GHz-band polarizer has realized excellent performance without tuning elements, i.e., the VSWR less than 1.06 and the axial ratio less than

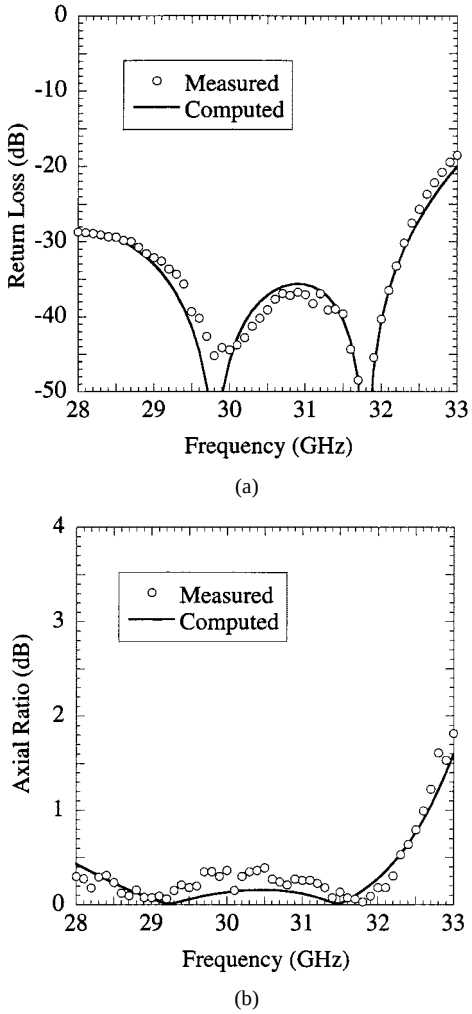

Fig. 8. Measured and calculated characteristics of the 30-GHz-band grooved circular waveguide polarizer. (a) Return loss. (b) Axial ratio.

0.3 dB over the frequency range between 20.0 and 21.5 GHz. The fabricated 30-GHz-band polarizer has also realized high performance without tuning elements, i.e., the VSWR less than 1.06 and the axial ratio less than 0.5 dB over the frequency range between 29.0–32.0 GHz. The above results verified the high efficiency of this design method.

V. Conclusion

A configuration, analysis, and design of grooved circular waveguide polarizers have been introduced in this paper. The presented polarizers are suitable for realizing high performance and low fabrication cost in the Ka-band and above because of the simple structure. The design method of the polarizers has applied the well-known design method of the branch waveguide coupler, and the design has been performed by the full-wave analysis of circular-to-rectangular waveguide H-/E-plane T-junction/cross junctions using mode-matching techniques. 20- and 30-GHz-band grooved circular waveguide polarizers fabricated with the aid of the analysis and design techniques have realized excellent performance without tuning elements. The theory has been verified by a good agreement with measurements.

References

[1] T. Kitsuregawa, *Advanced Technology in Satellite Communication Antennas: Electrical and Mechanical Design*. Norwood, MA: Artech House, 1990, pp. 81–86.
[2] J. Uher, J. Bornemann, and U. Rosenberg, *Waveguide Components for Antenna Feed Systems: Theory and CAD*. Norwood, MA: Artech House, 1993, pp. 417–435.
[3] J. Reed, "The multiple branch waveguide coupler," *IEEE Trans. Microwave Theory Tech.*, vol. MTT-6, pp. 398–403, Oct. 1958.
[4] G. Matthaei, L. Young, and E. M. T. Jones, *Microwave Filters, Impedance-Matching Networks, and Coupling Structures*. Norwood, MA: Artech House, 1964, pp. 809–819.
[5] N. Yoneda, M. Miyazaki, and T. Noguchi, "A 90-GHz-band monoblock waveguide orthomode transducer," in *IEEE MTT-S Int. Microwave Symp. Dig.*, 1999, pp. 1781–1784.
[6] E. Kuhn, "A mode-matching method for solving field problems in waveguide and resonator circuits," *Arch. Elektr. Uebertrag.*, vol. 27, pp. 511–518, Dec. 1973.
[7] T. Sieverding and F. Arndt, "Field theoretic CAD of open or aperture matched T-junction coupled rectangular waveguide structures," *IEEE Trans. Microwave Theory Tech.*, vol. 40, pp. 353–362, Feb. 1992.
[8] R. F. Harrington, *Time-Harmonic Electromagnetic Fields*. New York: McGraw-Hill, 1961, pp. 152–155.

Naofumi Yoneda (M'94) was born in Ehime, Japan, on May 12, 1964. He received the B.E., M.E., and Ph.D. degrees in electrical communication engineering from Tohoku University, Sendai, Japan, in 1988, 1990, and 1997, respectively.

In 1990, he joined the Mitsubishi Electric Corporation, Kamakura, Japan, where he has been engaged in research and development of antenna feeders and microwave and millimeter-wave circuits.

Dr. Yoneda is a member of the Institute of Electronics, Information and Communication Engineers (IEICE), Japan. He was the recipient of the 1991 Shinohara Award presented by the IEICE.

Moriyasu Miyazaki (M'92–SM'95) was born in Tokyo, Japan, on July 3, 1959. He received the B.E. degree in electrical engineering, and the M.E. and Ph.D. degrees in electronic engineering from Chiba University, Chiba, Japan, in 1982, 1984, and 1997, respectively.

In 1984, he joined the Mitsubishi Electric Corporation, Kamakura, Japan, where he has been engaged in research and development of antenna feeds and microwave circuits. He is currently a Team Leader in the Antennas Department, Information Technology Research and Development Center.

Dr. Miyazaki is a member of the Institute of Electronics, Information and Communication Engineers (IEICE), Japan.

Hiroyuki Matsumura was born in Tokyo, Japan, in 1962. He received the B.E. degree in electrical engineering from the Shonan Institute of Technology, Fujisawa, Japan, in 1984.

In 1984, he joined the Mitsubishi Electric Engineering Corporation, Kamakura, Japan, where he has been engaged in development and design of antennas for satellite installation.

Masao Yamato was born in Tokyo, Japan, in 1962. He received the B.E. degree in electronic engineering from Tohoku University, Sendai, Japan, in 1986.

In 1986, he joined the Mitsubishi Electric Corporation, Kamakura, Japan, where he has been engaged in development of antenna systems for telecommunication and satellite communication. He is currently an Assistant Manager in the Communications Engineering Section, Space Engineering Department, Kamakura Works.

Mr. Yamato is a member of the Institute of Electronics, Information and Communication Engineers (IEICE), Japan.